Stochastic Environmental Research and Risk Assessment 15 (2001) 87–100 © Springer-Verlag 2001

Application of the BME approach to soil texture mapping

D. D'Or, P. Bogaert, G. Christakos

Abstract. In order to derive accurate space/time maps of soil properties, soil scientists need tools that combine the usually scarce hard data sets with the more easily accessible soft data sets. In the field of modern geostatistics, the Bayesian maximum entropy (BME) approach provides new and powerful means for incorporating various forms of physical knowledge (including hard and soft data, soil classification charts, land cover data from satellite pictures, and digital elevation models) into the space/time mapping process. BME produces the complete probability distribution at each estimation point, thus allowing the calculation of elaborate statistics (even when the distribution is not Gaussian). It also offers a more rigorous and systematic method than kriging for integrating uncertain information into space/time mapping. In this work, BME is used to estimate the three textural fractions involved in a texture map. The first case study focuses on the estimation of the clay fraction, whereas the second one considers the three textural fractions (sand, silt and clay) simultaneously. The BME maps obtained are informative (important soil characteristics are identified, natural variations are well reproduced, etc.). Furthermore, in both case studies, the estimates obtained by BME were more accurate than the simple kriging (SK) estimates, thus offering a better picture of soil reality. In the multivariate case, classification error rate analysis in terms of BME performs considerably better than in terms of kriging. Analysis in terms of BME can offer valuable information to be used in sampling design, in optimizing the hard to soft data ratio, etc.

Key words: Bayesian maximum entropy, geostatistics, kriging, soil science, soil texture.

D. D'Or, P. Bogaert
Unité de Biométrie, Université Catholique de Louvain, Place Croix du Sud, 2 bte 16, B-1348 Louvain-la-Neuve, Belgium

G. Christakos
Environmental Modelling Program,
Department of Environmental Sciences and Engineering,
University of North Carolina,
Chapel Hill, 111 Rosenau Hall, CB#7400, NC, USA

Support was provided by grants from the Belgian National Fund for Scientific Research (FNRS), the US National Institute of Environmental Health Sciences (Grant no. P42 ES05948-02), the US Army Research Office (Grant no. DAAG55-98-1-0289) and the US Department of Energy (Grant no. DEFC09-93SR18262).

1
Introduction

In recent years, increasing attention has been paid to the problem of soil pollution and subsequent remediation procedures (e.g., Boulding, 1995; Asante-Duah, 1996). Authorities become aware of the fact that soil resources are scarce and have to be preserved for future generation (Dzombak et al., 1993). From a scientific point of view, this fact implies that efficient methods are needed to assess reliably the extent of the pollution and the risk incurred by neighbouring inhabitants.

Various methods of spatial analysis and estimation have been developed in the last few decades. From simple methods such as nearest neighbor, Delaunay tri-

angulation and inverse distance weighting, spatial analysis has evolved to the family of minimum mean squared error (MMSE) methods, including the various types of kriging (Agterberg, 1974; Arlinghaus, 1995; Olea, 1999). These methods use a linear combination of the available data to estimate the spatial distribution of the natural variable of interest and compute an estimation error variance. Kriging techniques, however, have some serious limitations, such as, an inability to account for important physical knowledge bases, and a conventional character lacking epistemic content. Also, underlying most kriging techniques is the Gaussian assumption, and in many cases (e.g., ordinary, simply and intrinsic kriging) the analysis is restricted to linear estimators. Moreover, recent types of kriging (e.g., indicator kriging) suffer from theoretical and practical problems (failing the monotonic cumulative distribution property, leading to unfeasible probability values, involving large numbers of kriging systems and variograms, etc.).

Accurate data being in most cases scarce or very expensive to acquire, new methods are needed for incorporating in a systematic and rigorous way a wider range of data types and scientific information, e.g., intervals, probability functions, engineering charts, and physical laws. The Bayesian maximum entropy (BME) approach introduced by Christakos (1990, 1992, 1998) provides a theoretically sound and physically meaningful method that is appropriate for such goals. The purpose of this work is to investigate BME's potential for estimating the soil textural fractions in space by integrating a small hard data set with a larger soft data set. The clay and sand contents are important factors for pollutant dynamics in the soil, influencing its water retention and adsorption capacity. Pedotransfer functions allow one to estimate the water retention curve in a soil and often take into account the percentage of clay or sand in the soil (Cosby et al., 1984; Vereecken et al., 1989). It is, thus, crucial to get the most accurate estimates possible for the textural fractions.

2
How soft data can improve estimation accuracy

2.1
The spatiotemporal random field concept

Most natural variables are assumed to vary continuously in space and time. From a stochastic viewpoint, the observed reality is considered to be just one realization of the natural variable among several other physically possible realizations. This consideration leads to the concept of spatiotemporal random field (S/TRF). Let $\mathbf{p} = (\mathbf{s}, t)$, where $\mathbf{s}$ denotes the spatial location vector and t the temporal coordinate. A S/TRF $X(\mathbf{p})$ is usually characterized by the mean function $m_x(\mathbf{p}) = \bar{X}(\mathbf{p})$, which expresses trends or systematic structures, and the covariance function $c_x(\mathbf{p}, \mathbf{p}') = E\{[X(\mathbf{p}) - \bar{X}(\mathbf{p})][X(\mathbf{p}') - \bar{X}(\mathbf{p}')]\}$, which represents

spatiotemporal interactions and dependencies. (In this work, capital English letters, e.g., X, will denote random fields, small English letters, e.g., x, will denote random variables and small Greek letters, e.g., χ, will denote their realizations.)

2.2 The BME analysis

When confronted with an environmental problem, soil scientists need to resort to various kinds of knowledge. They usually begin with their previous experience about similar situations, their knowledge of the laws of science, and their justified beliefs or assumptions regarding the natural phenomenon under consideration. These kinds of knowledge may be denoted as the "general knowledge base" G, since it is vague enough to characterize a large class of situations. On the other hand, scientists will also use data collected at the specific site, e.g., measurements of certain soil variables at points $\mathbf{p}_i$ $(i = 1, \ldots, m)$. This kind of knowledge will be denoted as "specificatory knowledge base" (or "case-specific knowledge base") S. The physical data χ_{data} of the S-base may be divided into two main groups: (i) *Hard data*, consisting of the available exact measurements of the natural variable. A set of hard data is denoted $\chi_{\text{hard}} = (\chi_1, \ldots, \chi_{m_{\text{h}}})$, where χ_i is a realization of the variable at point p_i $(i = 1, \ldots, m_{\text{h}})$; (ii) *Soft data*, including intervals and probability functions. A soft data set is denoted as $\chi_{\text{soft}} = (\chi_{m_{\text{h}}+1}, \ldots, \chi_m)$. Several examples of soft data sets are given in Christakos (2000). Note that, in the mapping context the map vector $\chi_{\text{map}} = (\chi_{\text{hard}}, \chi_{\text{soft}}, \chi_k)$ includes the vector of unknown values χ_k of the natural variable $X(\mathbf{p}_k)$ at points $\mathbf{p}_k$. At these points, the value of the random field has to be estimated using the hard and soft data available within a local neighborhood. The union of the general and specificatory knowledge yields the total knowledge $K = G \cup S$ about the natural phenomenon of interest.

From an epistemic viewpoint, BME analysis involves three stages, namely, the prior (or G) stage, the meta-prior (or S) stage, and the posterior (or integration K) stage.

2.2.1 Prior stage

At the prior stage, only knowledge available prior to any measurement is considered; in other words, only the G-base is used. The goal of this stage is to maximize the information content of the model given G. Let $f_G(\chi_{\text{map}})$ denote the G-based (prior) probability density function (pdf) of the random vector $\mathbf{x}_{\text{map}} = (x_1, \ldots, x_m, x_k)$ before any case-specific data have been taken into consideration. Mathematically, one seeks to maximize the expected map information

$$E[\text{Info}(\mathbf{x}_{\text{map}})] = -\int \ln[f_G(\chi_{\text{map}})]\, f_G(\chi_{\text{map}}) \mathrm{d}\chi_{\text{map}} \ , \tag{1}$$

subject to the physical constraints issued from the G-base. In many cases, these constraints can be expressed as

$$E[g_\alpha] = \int g_\alpha(\chi_{\text{map}}) f_G(\chi_{\text{map}}) \mathrm{d}\chi_{\text{map}} \ , \tag{2}$$

where the form of the g_α function depends on the kind of G-knowledge available. Simple examples of such functions are the moments of order one and two and the normalization constraint (Serre and Christakos, 1999),

$$g_0(\chi_{\text{map}}) = 1 \Rightarrow E[g_0] = 1 \quad \text{(normalization constraint)} \ , \tag{3}$$

$$g_\alpha(\chi_i) = x_i \Rightarrow E[g_\alpha] = E[x_i] \quad (\alpha = 1, \ldots, m+1) \quad \text{(mean at point } p_i) \ , \tag{4}$$

$$g_\alpha(\chi_i, \chi_j) = [\chi_i - \bar{x}_i][\chi_j - \bar{x}_j] \Rightarrow E[g_\alpha] = E[[x_i - \bar{x}_i][x_j - \bar{x}_j]], \tag{5}$$
$$(\alpha = m+2, \ldots, (m+1)(m+4)/2) \quad \text{(covariances } c(x_i, x_j)) \ .$$

Constraints resulting from higher-order moments like kurtosis and skewness, constraints related to the variogram model or to certain multiple-point statistics can be also considered. The solution to the maximization problem (1) leads to the following general expression for the *G*-based multivariate pdf

$$f_G(\chi_{\text{map}}) = Z^{-1} \exp\left[\sum_{\alpha=1}^{N_c} \mu_\alpha g_\alpha(\chi_{\text{map}})\right] \ , \tag{6}$$

where the partition function Z and the multipliers μ_α are found from the solution of the system of BME equations

$$Z = \int \exp\left[\sum_{\alpha=1}^{N_c} \mu_\alpha g_\alpha(\chi_{\text{map}})\right] \mathrm{d}\chi_{\text{map}} \ , \tag{7}$$

$$E[g_\alpha] = Z^{-1} \int g_\alpha(\chi_{\text{map}}) \exp\left[\sum_{\alpha=1}^{N_c} \mu_\alpha g_\alpha(\chi_{\text{map}})\right] \mathrm{d}\chi_{\text{map}} \ . \tag{8}$$

2.2.2
Meta-prior stage

At the meta-prior stage, case-specific data are collected and organized, which include hard and interval (soft) data, thus leading to the specificatory knowledge base *S*.

2.2.3
Integration or posterior stage

At this stage, the pdf is updated in the light of the *S*-base considered at the meta-prior stage, leading to the *K*-based pdf (Christakos and Li, 1998)

$$f_K(\chi_k) = A^{-1} \int_I f_G(\chi_{\text{map}}) \mathrm{d}\chi_{\text{soft}} \ , \tag{9}$$

where $A = \int_I f_G(\chi_{\text{data}})\, \mathrm{d}\chi_{\text{soft}}$ is a normalization coefficient and I is the domain of the interval (soft) data vector χ_{soft}. Different expressions of the posterior pdf are associated with different kinds of soft data (e.g., probability, functional or fuzzy data). Equation (9) is sometimes viewed as an information-processing rule.

2.3
BME mapping

The prior, *G*-based pdf (6) is substituted into the information-processing rule (9) of the integration stage, thus leading to the following expression for the posterior, *K*-based pdf of the map

$$f_K(\chi_K) = (AZ)^{-1} \int_I \exp\left[\sum_{\alpha=1}^{N_c} \mu_\alpha g_\alpha(\chi_{\text{map}})\right] \mathrm{d}\chi_{\text{soft}} \ , \tag{10}$$

where $\alpha = 1, \ldots, N_c$. Equation (10) offers a complete stochastic characterization of the map at point p_k. Specific estimates can be derived from this pdf. For example, the BME mode estimate $\hat{\chi}_k$ at point p_k is obtained by maximizing the posterior pdf (10) with respect to $\chi_k = \hat{\chi}_k$ which yields the BME mode equation below

$$\int_I \left\{ \exp\left[\sum_{\alpha=1}^{N_c} \mu_\alpha g_\alpha(\chi_{\text{map}})\right] \frac{\partial \sum_{\alpha=1}^{N_c} \mu_\alpha g_\alpha(\chi_{\text{map}})}{\partial \chi_k} \right\}_{\chi_k = \hat{\chi}_k} \mathrm{d}\chi_{\text{soft}} = 0 \ . \tag{11}$$

Note that the solution $\hat{\chi}_k$ obtained from Eq. (11) is, generally a nonlinear function of the data. Other estimates (like the median or the conditional mean) can be also derived from Eq. (10).

In the following, soil maps are produced from the combination of hard and soft data sets. Hard data are usually collected as full profile description, i.e., the horizons of a soil profile are first visually described (number of horizons, name, texture, structure, color, depth, etc.). Then samples from each horizon are analyzed for several variables (particle size, content in various chemical elements, CEC, etc.). Soft data usually come from auger boring, remote sensing or other sources (but no laboratory analyses). The goal of this work is to evaluate the performance of BME as a tool for incorporating soft data in soil texture mapping. The two case studies presented here deal with simulations. This allows us to compare under controlled conditions the soil maps generated from BME and geostatistical kriging techniques with the simulated soil map (which, for the purpose of the present analysis is assumed to be the actual/reference map).

3
Univariate case: estimation of the clay content

3.1
Clay content simulation maps

Clay content data were collected and analyzed at the Dinant region (Belgium). The theoretical covariance model fitted to these data was of the exponential form with a sill of $35.65\%^2$ and a range of 4000 m. A sequential Gaussian simulation of the clay content in the top horizon was performed on a 100×100-nodes grid (the distance between two adjacent nodes is 160 m). The simulated clay content map is plotted in Fig. 2c. This map will be considered as the actual map and will serve as a reference for comparisons.

3.2
Sampling strategy

Hard data (complete soil profile descriptions) were collected at arbitrary locations throughout the region, while interval (soft) type data (e.g., from a soil map or from auger borings) were collected on a grid. This sampling strategy is consistent with soil survey practice. In particular, soft data were generated by classifying the clay content into 10 interval classes, i.e., 0–10, 10–20,. . .,90–100%, and assuming that the actual (but unknown) values at each point lies within these intervals.

Using this sampling strategy, the reference map was sampled, yielding 148 arbitrarily located hard data points and 1156 soft data points located on the 160 × 160 m grid. These hard and soft data sets were used to derive the estimated soil maps.

3.3
Estimation strategy and comparisons

Based on the 148 hard data points available, the spatial structure of the clay content was represented by the experimental variogram (Fig. 1). A spherical model was fitted to this experimental variogram with a sill of 39.23 $(\%)^2$ and a range of 6850 m. On the basis of the hard and soft data sets, estimates were obtained at 10,000 simulation points using the SK and the BME techniques. The two sets of estimates were compared with the simulated values (Fig. 2c) in terms of: (i) the mean error (ME; which offers a measure of the estimation bias); (ii) the mean squared error (MSE; which is used as a measure of precision); and (iii) the error distribution (which globalizes the two former characteristics and adds information about the probability of identifying the actual value).

3.4
Results and discussion

Figure 2 shows the maps of the SK and BME estimates, as well as the reference map. The BME map is a better estimation of the reference map than the SK map. Detailed features are well identified by BME, while they are strongly smoothed out by SK (e.g., with SK, only the zones of extreme low or high values can be seen). Table 1 summarizes the ME and MSE results for BME and SK. The ME of the BME and SK estimates are not significantly different from zero, indicating that the two estimators are unbiased, as we expected from theory. The lower MSE for BME

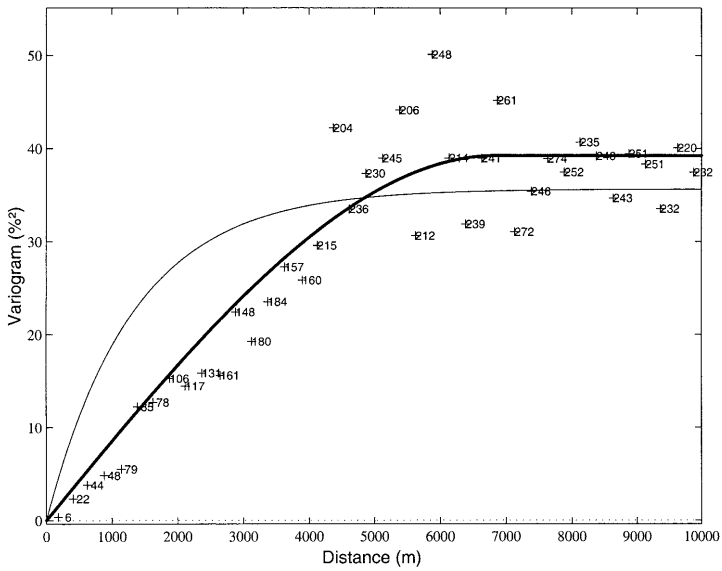

Fig. 1. Experimental variogram of the clay content (crosses), theoretical model (thin line) and fitted experimental model (bold line). The number of couples of points used for estimation is indicated next to each point. Clay content is expressed in % of the total soil composition

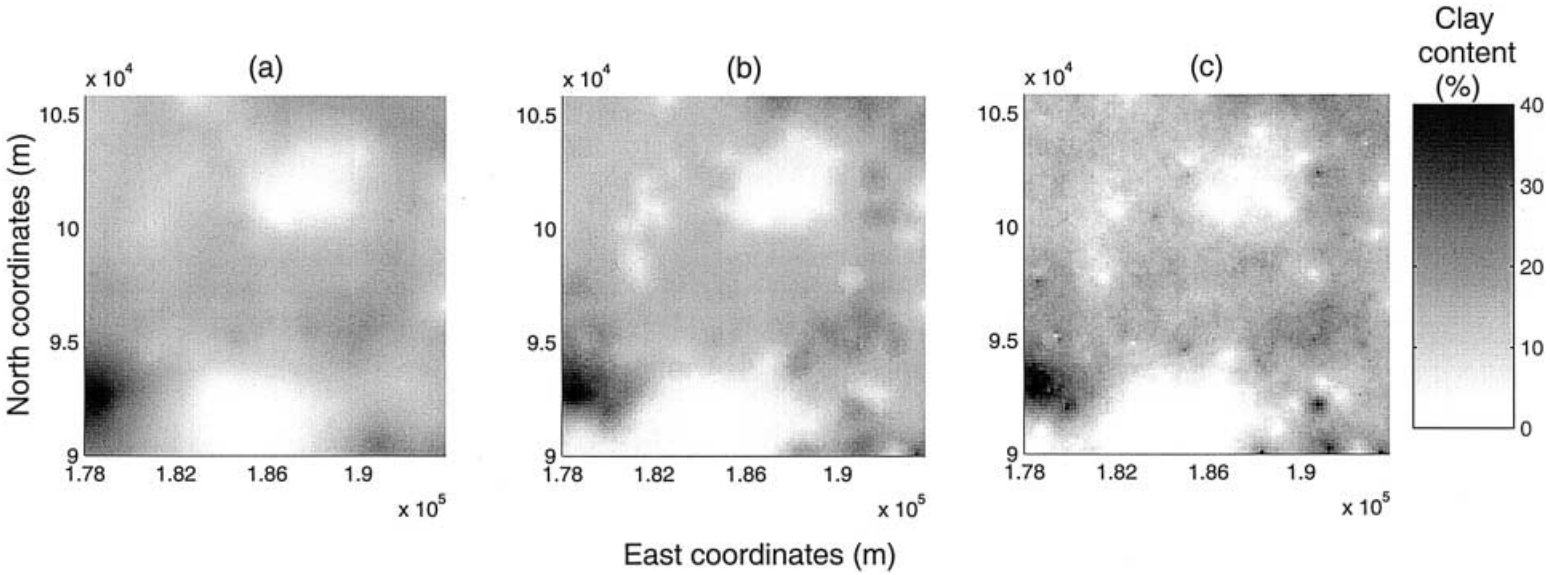

Fig. 2. **a** Map of SK estimates of the clay content, **b** map of BME estimates, and **c** reference map

Table 1. Mean error (ME) and mean squared error (MSE) for BME and SK, expressed as the proportion of clay in the total soil composition, in %

	BME	SK
ME	−0.0743	−0.3295
MSE	2.8199	10.9342

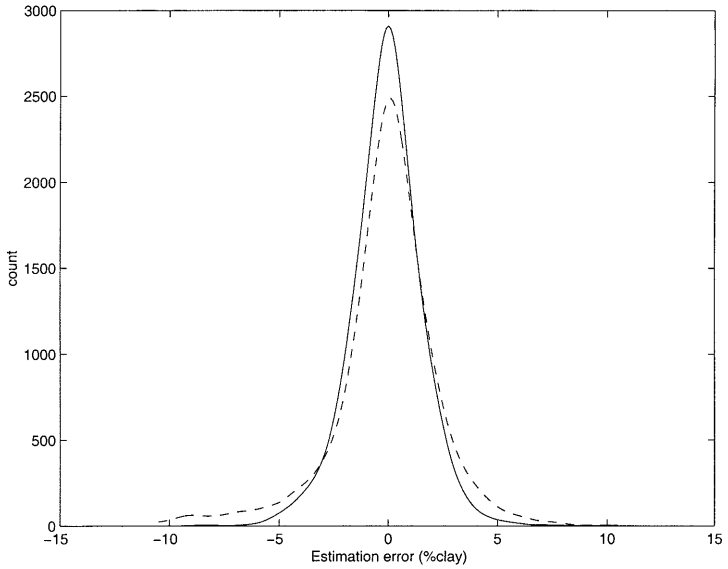

Fig. 3. Clay content estimation error distributions for BME (plain line) and SK (dashed line)

compared to SK indicates a higher accuracy of the estimates. Globally, BME is more accurate than SK, reflecting the important contribution of the soft data to the reduction of the estimation error. The shape of the estimation error distribution confirms these assessments (Fig. 3). The peak of the BME estimation error distribution is higher than that of SK, indicating a higher probability of obtaining an estimation error close to zero.

The improvement in spatiotemporal mapping accuracy gained by BME, compared to traditional kriging methods, is due to BME's ability to effectively take into account the knowledge contained in the soft data. While SK is based only on the 148 hard data points, BME makes good use of the 1156 soft data points, as well. The larger the ratio of soft to hard data is, the better the BME map will be compared to the SK map.

4
Multivariate case: the joint estimation of the three textural fraction (sand, silt and clay)

4.1
Simulation maps

The simulation scheme is the same as in the univariate case above. A sequential Gaussian co-simulation algorithm was run at the 10,000 nodes of the 160 × 160 m

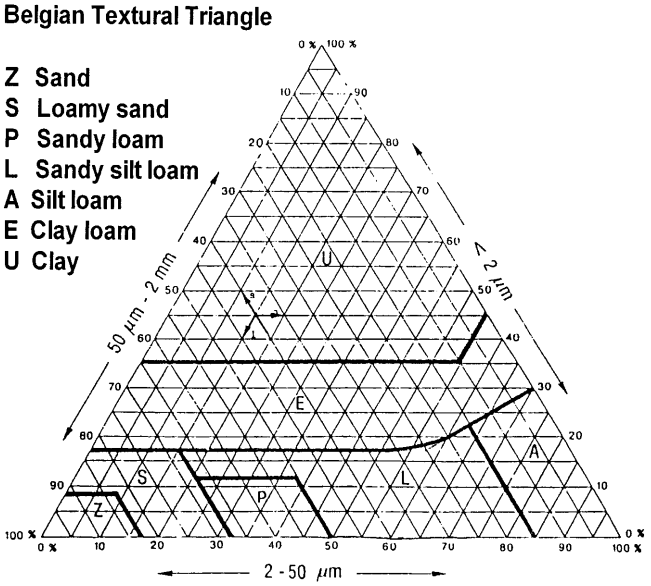

Fig. 4. Belgian textural triangle providing the soil type as a function of the three textural fractions (expressed in %)

grid. The theoretical variogram model is exponential with a range of 1600 m and the following covariance matrix:

$$\begin{bmatrix} 90.79 & -86.34 & -4.09 \\ -86.34 & 115.97 & -29.46 \\ -4.09 & -29.46 & 33.74 \end{bmatrix} .$$

One map was obtained for each fraction (sand, silt and clay). Furthermore, a classification was performed according to the textural triangle of the Belgian soil classification (Fig. 4). In this way, a soil map could be built from the knowledge of the textural fractions. Figure 6c represents the simulated textural units and will be used as the reference map.

4.2 Sampling strategy

Following the same philosophy as in the univariate case above, 150 hard data points were selected at random, and 1134 soft data points were sampled on a grid for each one of the three fractions. According to the textural soil diagram shown in Fig. 4, for each textural fraction the boundaries of the soil class to which the soft data points belong were taken as values of the bounds for the soft data intervals. A linear model of coregionalization (LMC) was then estimated from the 150 hard data points. An exponential model was fitted to the experimental (cross-) variograms with a range of 3500 m and the following covariance matrix:

$$\begin{bmatrix} 110.45 & -100.74 & -9.46 \\ -100.74 & 134.59 & -33.63 \\ -9.46 & -33.63 & 43.35 \end{bmatrix} .$$

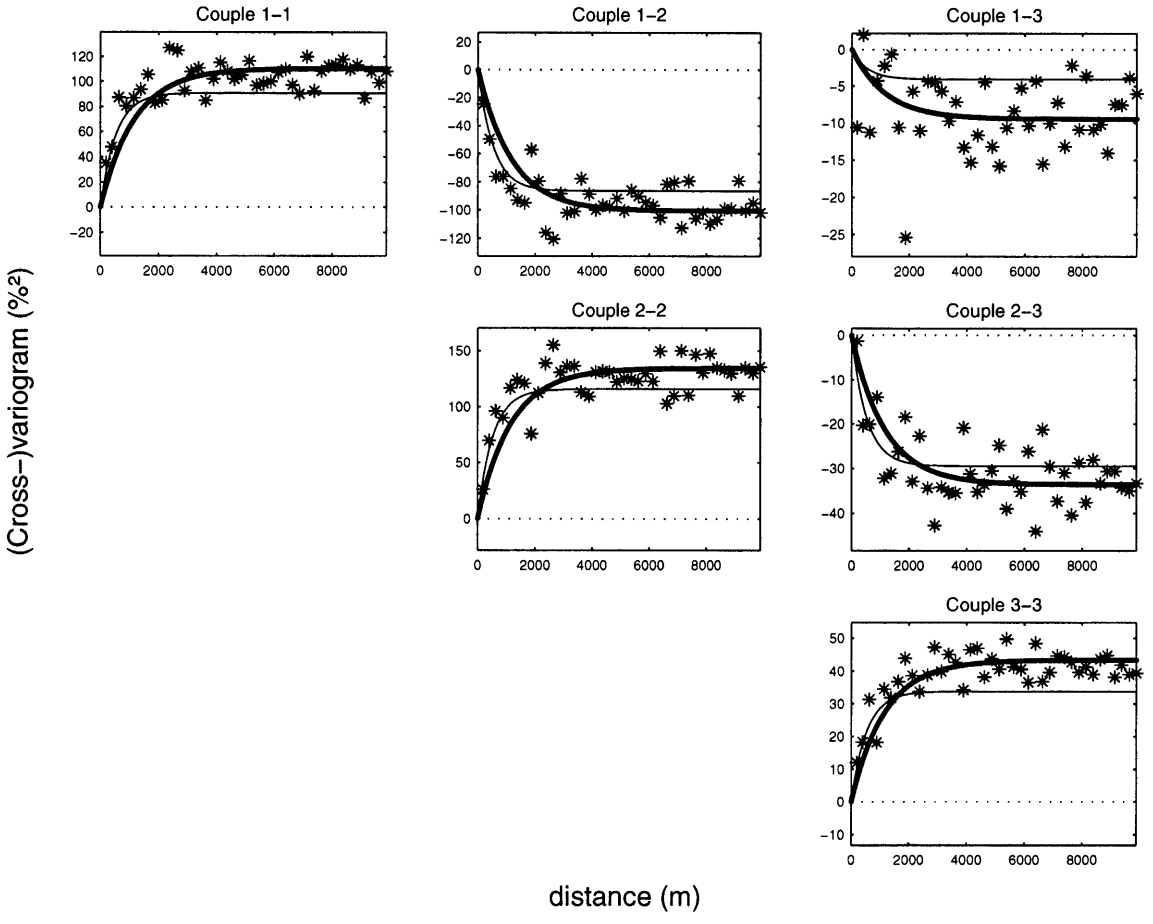

Fig. 5. Experimental (cross-) variograms for the three textural fractions; theoretical model (thin line), and fitted experimental model (bold line)

Figure 5 shows the experimental (cross-) variograms, as well as the theoretical and fitted experimental models.

4.3
Estimation strategy and comparisons

Estimated soil maps were drawn after classifying each point of the spatial region according to the textural triangle on the Belgian soil classification (Fig. 4). As in the univariate case, the estimates obtained from the BME and SK methods were compared to the reference map in terms of the ME, MSE, and estimation error distributions. In addition to these comparisons, the classification error rate was used to compare the estimated soil maps with the reference soil map.

4.4
Results and discussion

Figure 6 shows the BME and SK soil maps, as well as the reference soil map. Clearly, the BME map is much more accurate and informative than the SK map; e.g., the BME map identifies small zones and the contours of the soil units are well reproduced (SK, on the other hand, seems to offer a poor representation of the same contours).

To confirm these visual impressions numerically, the rate of classification error was calculated. This rate is defined as the percentage of estimation points for which the estimated soil class was different from the reference class. SK was found to have a classification error rate of 43.25%, while BME attributes a false texture class to only 30.08% of the estimation points. The benefit of using BME is significant, but could have been further improved if a greater number of texture classes had been considered in this study. Not surprisingly, the MSEs for the three textural fractions are smaller for BME than for the SK (Table 2), thus indicating that BME reduces the range of the estimation error distribution. As in the univariate case, BME increases the probability of an error close to zero (see, Fig. 7). The smaller difference observed between BME and SK in the case of clay content is a result of the data configuration on the textural triangle. Indeed, for the clay fraction, both the soft and the hard data are covering the entire range of possible values, and as a consequence soft data do not bring so much new information (in addition to the hard data). For the loam and sand fractions, on the other hand, each of the hard and the soft data sets cover only a part of the range of values. Therefore, using only hard data, SK introduces a bias in the estimation. At the same time, by using the additional soft (interval) data, BME is able to moderate the bias. This fact demonstrates that, depending on the kind of information

Table 2. Mean error (ME) and mean squared error (MSE) for the sand, silt and clay fractions. Errors for three textural fractions are expressed as a proportion of the total soil composition in %

Textural fraction		BME	SK
Sand	ME	1.28	0.33
	MSE	53.66	80.42
Silt	ME	−1.33	−0.74
	MSE	63.09	98.77
Clay	ME	0.05	0.41
	MSE	17.89	23.89

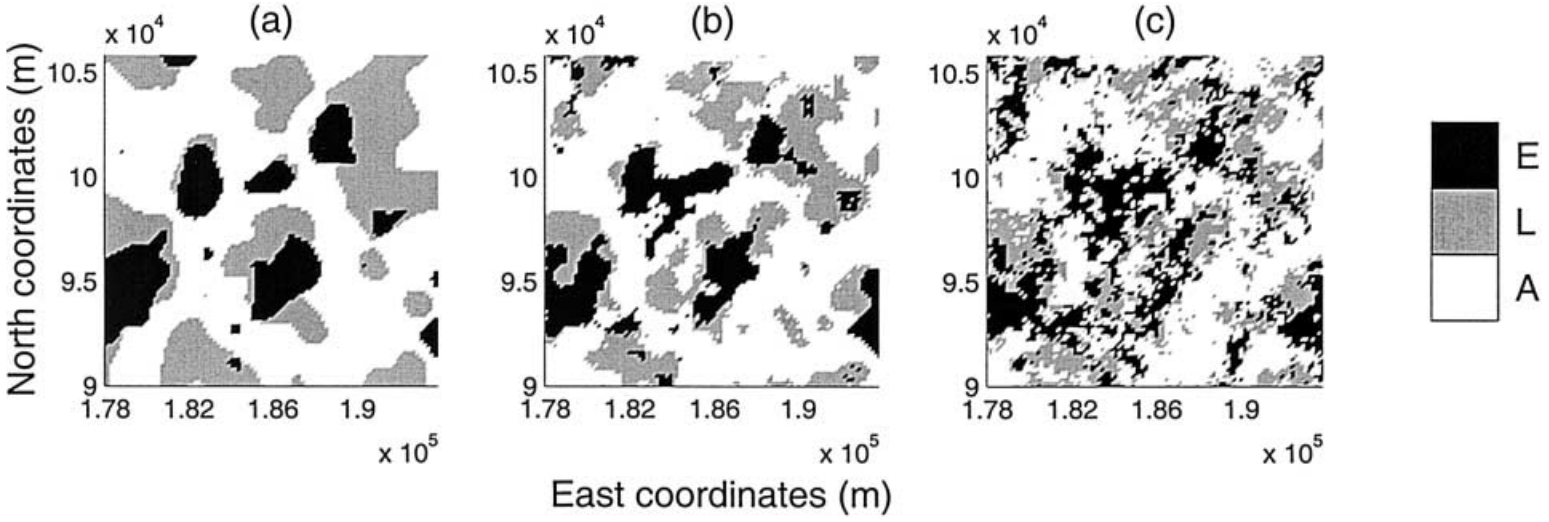

Fig. 6. **a** SK map, **b** BME map, and **c** reference soil map of the soil type. Soil symbols (A, L, E) refer to the textural triangle (Fig. 4)

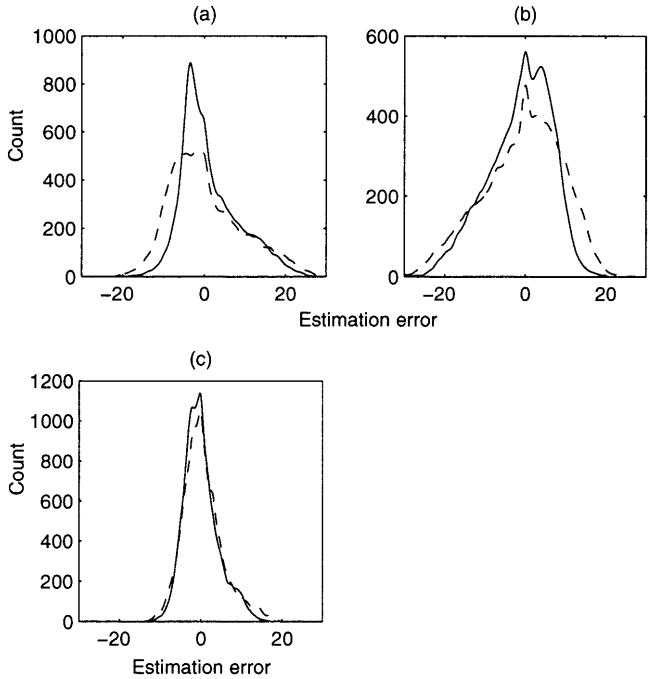

Fig. 7. Estimation error distributions for **a** sand, **b** silt, and **c** clay fractions using BME (plain line) and SK (dashed line)

contained in the soft data, the way BME incorporates soft data can have a significant impact on the accuracy of the estimation results. It should be noted that the use of the specific transformation for compositional data – as recommended by Aitchinson (1986, 1997) – does not change significantly the results of the analysis.

5
Conclusions

The two case studies presented here demonstrated that BME is a powerful method for incorporating uncertain physical knowledge bases in the mapping process. In both cases, the maps produced by BME offered much better representations of the actual (simulated) maps than the maps obtained by a kriging method (e.g., the contours were defined with greater precision by BME, and small zones were better identified by BME than by SK). These visual assertions were corroborated in terms of numerical comparisons involving MSE and ME statistics. While none of the methods was found to be biased, BME produced smaller estimation errors than SK. The estimation error distributions clearly showed that BME leads to a higher probability of having an estimation error close to zero than SK. BME is an efficient estimator in cases where hard data are scarce or expensive to collect. This situation is often encountered in environmental sciences, where the lack of hard data can be compensated for by the use of soft data. Soft data are usually available in great quantities using cheaper methods, from existing databases or maps, or from experts who have dealt with similar situations. Moreover, unlike kriging methods, BME does not make any restrictive assumptions about the normality of the underlying distribution, and provides the complete pdf at each estimation point. This allows the efficient computation of the estimation variances, quantiles

and confidence intervals, which are useful indicators in risk assessment studies. In soil sciences, where the texture information obtained from the soil map is frequently used, BME could be of great help in estimating the sand, silt and clay contents. The accurate estimation of these three variables can have a significant influence on the accuracy of the results produced by soil process models (pollutant leaching, irrigation or erosion models, etc.).

Future work should focus on a number of areas. While in this work we considered single-point BME analysis of soil data, one should also evaluate the advantages of using multi-point BME (i.e., simultaneous estimation at several points). BME can easily incorporate multiple-point statistics, which in certain cases reveal important features of the soil variable. In the case of pollutant leaching problems, e.g., one should evaluate the benefits of using BME instead of SK to estimate the textural fractions, thus increasing the accuracy of estimates of the amount of pollutant reaching the water table. Furthermore, BME could be helpful to environmental scientists seeking to optimize a sampling design, or to determine the nest ratio of hard to soft data (especially in cases of limited sampling budgets). Also, BME can be a valuable tool in automatic soil mapping, as it provides a sound theoretical and operational way to combine, integrate and interpret data from various sources (e.g., data from an existing soil map, land cover data from satellite pictures, and digital elevation models). It is hoped that the promising results obtained in this work will stimulate further research on the application of BME analysis in the fields of soil science and engineering.

References

Agterberg FP (1974) Geomathematics. Elsevier Scientific Publ., Amsterdam, the Netherlands

Aitchinson J (1986) The Statistical Analysis of Compositional Data. Chapman & Hall, London

Aitchinson J (1997) The one-hour course in compositional data analysis or compositional data analysis is simple. Proceedings of the IAMG'97 (Barcelona), 3–35

Arlinghaus SL (ed.) (1995) Practical Handbook of Spatial Statistics. CRC Press, New York

Asante-Duah DK (1996) Management of Contaminated Site Problems, CRC Lewis Publ., Boca Raton, FL

Boulding JR (1995) Practical Handbook of Soil, Vadose Zone, and Groundwater Contamination. CRC Lewis Publ., Boca Raton, FL

Christakos G (1990) A Bayesian/maximum-entropy view to the spatial estimation problem. Math. Geol., 22(7): 763–777

Christakos G (1992) Random Fields Models in Earth Sciences. Academic Press, San Diego, CA

Christakos G (1998) Spatiotemporal information systems in soil and environmental sciences. Geoderma, 85(2–3): 141–179

Christakos G, Li X (1998) Bayesian maximum entropy analysis and mapping: A farewell to kriging estimators? Math. Geol., 30(4): 435–462

Christakos G (2000) Modern Spatiotemporal Geostatistics. Oxford University Press, New York

Cosby BJ, Hornberger GM, Clapp RB, Ginn TR (1984) A statistical exploration of soil moisture characteristics. Water Resour. Res., 24: 755–769

Dzombak DA, Labience PA, Siegrist RL (1993) The need for uniform soil cleanup goals, Environ. Sci. Technol., 27: 765–766

Olea RA (1999) Geostatistics for Engineers and Earth Scientists. Kluwer Academic Publishers, Boston, MA

Serre ML, Christakos G (1999) Modern geostatistics: computational BME analysis in the light of uncertain physical knowledge – the Equus Beds study. Stochastic Environ. Res. Risk Assessment 13(1): 1–26

Vereecken H, Maes J, Feyen J, Darius P (1989) Estimating the soil moisture retention characteristics from texture, bulk density and carbon content. Soil Sci., 148: 389–403